Pergamon

Fe isotopic fractionation during mineral dissolution with and without bacteria

Susan L. Brantley,[1,*] Laura J. Liermann,[1] Robin L. Guynn,[1] Ariel Anbar,[2] Gary A. Icopini,[1] and Jane Barling[2]

[1]The Pennsylvania State University, Department of Geosciences, University Park, PA 16801, USA
[2]University of Rochester, Department of Earth and Environmental Sciences, Rochester, NY 14627, USA

Abstract—Fe released into solution is isotopically lighter (enriched in the lighter isotope) than hornblende starting material when dissolution occurs in the presence of the siderophore desferrioxamine mesylate (DFAM). In contrast, Fe released from goethite dissolving in the presence of DFAM is isotopically unchanged. Furthermore, $\Delta^{56}Fe_{solution\text{-}hornblende}$ for Fe released to solution in the presence of ligands varies with the affinity of the ligand for Fe. The extent of isotopic fractionation of Fe released from hornblende also increases when experiments are agitated continuously. The Fe isotope fractionation observed during hornblende dissolution with organic ligands is attributed predominantly to retention of ^{56}Fe in an altered surface layer, while the lack of isotopic fractionation during goethite dissolution in DFAM is consistent with the lack of an altered layer. When a siderophore-producing soil bacterium is added to the system (without added organic ligands), Fe released to solution from both hornblende and goethite differs isotopically from Fe in the bulk mineral: $\Delta^{56}Fe_{solution\text{-}starting\ material} = -0.56 \pm 0.19$ (hornblende) and -1.44 ± 0.16 (goethite). Increased isotopic fractionation is attributed in this case to the fact that as bacterial respiration depletes the system in oxygen and aqueous Fe is reduced, equilibration between aqueous ferrous and ferric iron creates a pool of isotopically heavy ferric iron that is assimilated by bacterial cells. Adsorption of isotopically heavy ferrous iron (Fe(II) enriched in the heavier isotope) or precipitation of isotopically heavy Fe minerals may also contribute to observed fractionations.

To test whether these Fe isotope signatures are recorded in natural systems, we also investigated extractions of samples of soils from which the bacteria were isolated. These extractions show variability in the isotopic signatures of exchangeable Fe and Fe oxyhydroxide fractions from one soil sample to another, but exchangeable Fe is observed to be lighter than Fe in soil Fe oxyhydroxides and hornblende. This observation is consistent with isotopically light Fe-organic complexes in soil pore water derived from the Fe-silicate starting materials in the presence of growing microorganisms, as documented in experiments reported here. The contributions from phenomena including organic ligand-promoted nonstoichiometric dissolution of Fe silicates, uptake of ferric iron by organisms, adsorption of isotopically heavy ferrous iron, and precipitation of iron minerals should create complex isotopic signatures in soils. Better understanding of these processes and the timescales over which they contribute to fractionation is needed.   *Copyright © 2004 Elsevier Ltd*

1. INTRODUCTION

Beard and Johnson (1999) showed that isotopic fractionation by dissimilatory iron-reducing bacteria can cause isotopic variations of ~1.3‰ when Fe^{2+} is released to solution during the reduction of ferrihydrite, and suggested this isotopic shift may represent a biosignature for microbial cycling of Fe. Brantley et al. (2001b) observed that Fe isotopes are also fractionated during hornblende dissolution in the presence of *Bacillus* sp. (first tentatively identified as *Arthrobacter* sp.) and *Streptomyces* sp. $\delta^{56}Fe$ of Fe released to solution in the presence of these bacteria showed values of -0.5 to -0.6‰ relative to the hornblende crystal. These findings suggest that Fe isotope fractionation may occur during biologically mediated mineral dissolution. In the same study, Fe isotope fractionation between dissolved Fe and Fe in the bulk mineral was also observed during *abiotic* hornblende dissolution in the presence of either oxalic acid or the siderophore desferrioxamine mesylate (DFAM) ($\Delta^{56}Fe_{solution\ -\ hornblende} = -0.25 \pm 0.18$ and -0.36 ± 0.25‰ respectively). These data suggested that Fe isotope fractionation during biologically mediated dissolution could be

explained at least partially by chelation, and that such fractionation is possible even in the absence of bacteria if siderophores or other strong Fe complexers are present. Siderophores, low-molecular weight organic molecules with high specificity for Fe^{3+}, are secreted by microorganisms to bind and take up Fe (e.g., Neilands, 1984; Hughes and Poole, 1989). Most siderophores are either catechols or hydroxamates (Neilands, 1984) with formation constants for ferric iron as high as 10^{51} (Hider, 1984; Hughes and Poole, 1989; Winkelmann, 1991; Hersman et al., 1995).

Ligand-associated effects may be ubiquitous in soil systems: a typical soil pore water might contain 1000 μM oxalic acid (Fox, 1990), 174 μM acetic acid (Fox, 1990), and 240 μM siderophores (Hersman et al., 1995), as well as trace malic, citric and succinic acid. Siderophores bind Fe^{3+} more effectively than do low molecular weight organic acids, especially at neutral to alkaline conditions. Large reservoirs of siderophores are adsorbed to soil organic matter; therefore, hydroxamate siderophores may perform many chelate functions previously attributed to organic acids and polyphenolic humic material in soils (Powell et al., 1980).

Siderophore and other Ligand effects may also be ubiquitous in oceanic systems. Much of the Fe in seawater is complexed, and natural Fe-binding ligands in seawater may be siderophores

* Author to whom correspondence should be addressed (brantley@essc.psu.edu).

Table 1. Hornblende crystal composition.[a]

Solid	Si (wt%)	Al (wt%)	Fe (wt%)	Mg (wt%)	Ca (wt%)	Na (wt%)	K (wt%)	Mo (ppm)	Ni (ppm)
Hornblende crystal	21.5	8.98	6.35	6.1	5.7	2.3	0.35	<1	110

[a] Measured by ICP-AES.

(see review by Macrellis et al., 2001). These marine siderophores may be stronger Fe binding ligands than terrestrial siderophores (Reid et al., 1993), and siderophores may be important in understanding bacterial responses in the recent Fe addition experiment in the eastern equatorial Pacific (Rue and Bruland, 1997, as reviewed by Macrellis et al., 2001). Despite the importance of siderophores in Fe cycling, siderophore-promoted dissolution of iron-containing minerals has only been infrequently investigated (Watteau and Berthelin, 1994; Hersman et al., 1995; Holmén and Casey, 1996, 1999; Kraemer et al., 1999; Liermann et al., 2000a,b; Kalinowski et al., 2000a,b; see also Stone, 1997), and the effect of siderophores on isotopic fractionation of Fe is not understood.

The cause of isotope fractionation during dissolution of Fe silicate in the presence of organic molecules is unclear. Brantley et al. (2001b) postulated a kinetic isotope effect during Fe-ligand surface complexation or during oxidation of Fe^{2+} to Fe^{3+}, but such effects have not been studied thoroughly. Both kinetic and equilibrium isotope effects have been identified in Fe fractionation, and so both are plausible (e.g., Anbar et al., 2000; Bullen et al., 2001; Matthews et al., 2001; Johnson et al., 2002; Roe et al., 2003).

In contrast, Johnson et al. (2002) have argued that Fe isotope effects during dissolution should be insignificant in the case of homogeneous dissolution of an isotopically homogeneous substrate as long as the rate of dissolution exceeds the rate of solid-state diffusion.

In this contribution, we extend the work of Brantley et al. (2001b) by examining Fe isotope fractionation during hornblende dissolution in the presence of citric or acetic acids. These experiments were conducted with and without constant agitation to vary the reactivity of surfaces. Furthermore, Fe^{2+} and Fe^{3+} were also measured for hornblende ± ligand ± bacteria experiments. In addition, we have conducted experiments using goethite instead of hornblende, dissolved with and without Bacillus sp. and DFAM. The mode of dissolution of goethite, a ferric oxide, is very different from that of hornblende, a chain silicate, and differences in observed isotopic effects provide insight into fractionation. Finally, we reinvestigate Fe on exchange sites and in oxyhydroxides in a hornblende-containing soil.

2. METHODS

2.1. Experimental Setup

2.1.1. Medium and bacteria

MM9 medium was used because it is a pH-buffered chemically defined bacterial medium (Kalinowski et al., 2000b). The medium was prepared by dissolving 6.0 g/L Na_2HPO_4, 0.3 g/L KH_2PO_4, 0.5 g/L NaCl, 1.0 g/L NH_4Cl, and 6.06 g/L Tris base ($C_4H_{11}NO_3$) in distilled deionized water. The pH was then adjusted to 7.4 using HCl and the solution autoclaved. The medium was supplemented with 2% (v/v) of

10% (w/v) casamino acids (Difco Laboratories), 0.2% 1 M $MgSO_4$, 1% (v/v) of 20% (w/v) glucose, and 0.01% (v/v) 1 M $CaCl_2$, which were prepared and sterilized separately (Maniatis et al., 1982; Schwyn and Neilands, 1987; Liermann et al., 2000a). Ultrapure components were used when available. Tris, glucose, and casamino acids solutions were treated in batch with Chelex cation exchange resin (Bio-Rad) before use to remove metals (Liermann et al., 2000a). All experiments were performed in the dark in a cabinet or unlighted incubator.

For biotic experiments, a bacterium isolated from a soil from Gore Mountain, NY was used. This organism, an oxygen-respiring heterotroph, was chosen because it grows robustly in Fe-poor medium in the presence of hornblende by producing siderophores. 16S rRNA gene sequencing performed on the organism revealed that it most closely resembles a strain of Bacillus mycoides (similarity rank 0.986, Nucleic Acid Facility, Life Sciences Consortium, The Pennsylvania State University). The organism will be referred to here as a species of Bacillus (Bacillus sp.) The organism was previously identified as a species of Arthrobacter based on partial 16S rRNA sequencing (Kalinowski et al., 2000b; Liermann et al., 2000a,b; Brantley et al., 2001a; Brantley et al., 2001b).

2.1.2. Hornblende experiments

These experiments were designed to extend the observation of Brantley et al. (2001b) that organic ligands fractionate Fe isotopes during leaching of hornblende. In the earlier experiments, we used MM9 medium, a different batch of hornblende powder (specific surface area = 0.17 $m^2\ g^{-1}$), oxalic acid, and desferrioxamine mesylate (DFAM) as ligands. Following our earlier methods, hornblende experiments were conducted at 20–25°C in 250 mL glass flasks, capped with aluminum foil.

The hornblende crystal (collected from Gore Mountain, NY; composition summarized in Table 1) was crushed and sieved (250 to 350 μm), then rinsed and sonicated extensively with acetone to remove fine particles. Ultrapure acetone was used for the final two rinses, and powder was then dried. Although the batch of hornblende was collected from the same location and prepared similarly to the procedure used previously (Brantley et al., 2001b), we produced a powder with a slightly different specific surface area: 0.19 m^2/g (N_2 BET, Micrometrics ASAP 2000).

Bacillus sp. were grown in 5–10 mL MM9 medium to late log-stationary phase on a tabletop shaker; 100 μL aliquots were used to inoculate experimental cultures.

Flasks were run with 60 mL MM9 medium and 2 g hornblende powder ± bacteria ± organic ligands. 24 μM concentration of the following ligands (Table 2) were used: acetate (number of flasks, n, = 3), oxalate (n = 2), citrate (n = 3), and DFAM (n = 2). Two separate sets of flasks were also set up (n = 3, n = 2) to contain only the bacterial medium and hornblende. All flasks were agitated manually

Table 2. Ligands.

Ligand	Expression for K	Log K[a]
Water	$[FeOH^{2+}][H^+]/[Fe^{3+}][H_2O]$	−2.9
Acetic acid	$[FeCH_3COO^{2+}]/[Fe^{3+}][CH_3COO^-]$	3.2
Oxalic acid	$[FeC_2O_4^+]/[Fe^{3+}][C_2O_4^{2-}]$	7.6
Citric acid	$[FeC_6H_5O_7]/[Fe^{3+}][C_6H_5O_7^{3-}]$	11.4
DFAM	$[FeC_{25}H_{48}N_6O_8]/[Fe^{3+}][C_{25}H_{48}N_6O_8]$	30.7

[a] From NIST (1998).

once each day for approximately 10 s, before sampling. To test the importance of agitation, abiotic experiments with hornblende + citric or acetic acid were also prepared and sampled identically, but agitated constantly at 150 rpm in a tabletop shaker for 6 d.

A blank of MM9 medium ± organic ligand (i.e., no bacteria or mineral added) was sampled for all experiments to represent time 0. After brief manual agitation on days 1, 4, and 6, 10 mL samples were collected from the flasks using sterile pipettes and aseptic technique. Samples were filtered (0.2 μm), tested for pH, acidified with 1% (v/v) ultrapure HNO_3, and stored at 4°C before analysis.

2.1.3. Goethite experiments

One homogenized batch of goethite was synthesized and used for all experiments (Schwertmann and Cornell, 1991): 100 mL of 1 M $Fe(NO_3)_3$ was mixed with 180 mL of 5 M KOH solution, diluted to 2 L, and heated for 60 h at 70 C. Both salts were Mallinckrodt reagent grade (product numbers 5032 and 6984, respectively). The product was rinsed extensively with distilled-deionized water and dried at 30°C. The identity was confirmed by X-ray diffraction analysis. Surface area determined by N_2 BET (Micrometrics ASAP 2000) was 31 m^2/g.

Goethite experiments were conducted in triplicate with medium volumes of either 60 or 110 mL, but with a constant ratio of 100 to 1 of medium volume (ml) to mineral mass (g). All experiments were conducted in glass flasks capped with aluminum foil agitated manually once each day. Solution was sampled as described for hornblende experiments.

2.3. Analyses

2.3.1. Concentrations

Concentrations of dissolved Fe were analyzed by high resolution inductively coupled plasma mass spectrometry (HR-ICP-MS) (Finnigan MAT Element I). All solution samples were diluted 1:20 and acidified to 1% HNO_3 for analysis.

Repeated analysis of standard solutions across all runs shows that the accuracy and precision of analysis across different runs is better than ±13%. The detection limits for all elements other than Si were approximately 0.1 μM. Because of high background levels, the detection limit for Si was approximately 2 μM.

To measure the concentration of Fe^{2+} in some flasks, 1 mL aliquots were immediately filtered (0.2 μm) into a cuvette containing 100 μL HCl. Two mL of buffered ferrozine solution was added, allowed to react for several minutes; and then the absorbance at 562 nm was measured spectroscopically (Lovely and Phillips, 1986). The detection limit (0.18 μM) was estimated by analyzing dilute standard solutions. For concentrations ≤0.18 μM, absorbance readings were indistinguishable from MM9 medium without added Fe.

2.3.2. Fe isotopes

Fe isotope measurements were conducted using either the Plasma 54 (VG Elemental) MC-ICP-MS at the University of Rochester or the Neptune MC-ICP-MS at the ThermoFinnigan facility in Bremen, Germany. To prepare for isotopic analysis, a sample aliquot containing at least 6 μg of Fe was dried down to a bead in a Savillex vial on a hot plate, and then reacted with concentrated HNO_3 on a hot plate to oxidize most organic matter. The organic matter digestion in the capped vessel was allowed to continue until nitrous oxide fumes ceased to form. Once oxidation was complete, the sample was again dried to a bead and redissolved in 7 M HCl with a small amount of H_2O_2. This solution was loaded onto an anion exchange column (BioRad AG MP-1 resin; 0.8 cm diameter, 4 cm bed length) previously treated with 18 MΩ water (9 mL), 0.5 M HCl (5 mL), and 7 M HCl (9 mL) to clean and condition the resin. Matrix elements were separated from Fe in the sample by rinsing the loaded columns with 7 M HCl (27 mL). The Fe was then eluted with 0.5 M HCl (6 mL). Aliquots of the load and eluate solutions were analyzed for Fe concentration by isotope dilution to verify that yields were essentially quantitative. High yield through the anion exchange chemistry is necessary because of the potential for Fe isotope fractionation by this process (Anbar et al., 2000). The eluted

solution was dried down again and redissolved in 0.05 M HNO_3 for MC-ICP-MS analysis.

Mass spectrometry procedures (Anbar et al., 2000; Roe et al., 2003; Weyer and Schweiters, 2003; Arnold et al., 2004) are summarized below. Solutions were analyzed by MC-ICP-MS at a concentration of 2–3 ppm Fe with a Cu spike added to correct for instrumental mass bias following a procedure similar to that outlined in Maréchal et al. (1999) and Anbar et al. (2001). On the Plasma54, isobaric contributions from ArN^+ and ArO^+ at masses 54 and 56 respectively were minimized by using a desolvating nebulizer (Aridus I, CETAC). These interferences were monitored at the beginning of each analytical session and periodically thereafter. Interference from $ArOH^+$ at mass 57 was negligible. On the Neptune, data were collected in medium resolution mode. In this mode, the isobaric interferences are resolved sufficiently to permit interference-free isotope ratio measurements (Weyer and Schwieters, 2003). The Neptune methodology was validated by measuring samples previously characterized on the Plasma54. These samples included Fe extracted from hydrothermal fluids and an iron meteorite (Sharma et al., 2001). $\delta^{56}Fe$ values for these samples with both methodologies were identical with error at the 2σ level.

Sample solutions were analyzed at least twice, along with two standards (an ICP Fe standard, and a gravimetric Fe standard), also in 0.05 mol/L HNO_3 containing Fe at the same concentration as the samples. Fe isotope values reported here are the means of these replicate measurements. The ratios $^{56}Fe/^{54}Fe$ and $^{57}Fe/^{54}Fe$ were measured simultaneously; analyses that did not demonstrate the expected mass-dependent relationship between these ratios were rejected.

By convention, $\delta^{56}Fe$ values are presented relative to the international IRMM standard (Eqn. 1):

$$\delta^{56}Fe = [(^{56}Fe/^{54}Fe_{sample}/^{56}Fe/^{54}Fe_{IRMM}) - 1] \times 1000 \qquad (1)$$

This represents a change in reporting standard from the BIR standard used in Brantley et al. (2001b); the IRMM standard is ~ 0.09‰ lighter than the BIR standard used previously. The external precision of measurements (1σ) was better than ± 0.15‰ on the Plasma54 and ±0.05‰ on the Neptune (Weyer and Schwieters, 2003; Arnold et al., 2004).

2.4. Soil Extractions

The B horizon of a hornblende-containing soil from Gore Mountain New York was also sampled for isotopic analysis. Exchangeable Fe was removed from the soil using the same procedure as used previously (Brantley et al., 2001b), by adding 30 mL of 1 M $MgCl_2$ to 0.5 g of air-dry soil. The mixture was shaken for 2 h, then filtered and the filtrate acidified to 1% HNO_3 for analysis (Hendershot et al., 1993). Fe oxides were also extracted from the sample soil by adding 25 mL of 0.68 mol/L sodium citrate and 0.4 g of sodium dithionite to 0.5 g of air-dry soil. The mixture was shaken for 17 h then filtered and the filtrate acidified for analysis (Hendershot et al., 1993).

3. RESULTS

3.1. Aqueous Chemistry vs. Time

In flasks containing no bacteria with or without organic ligands, the pH generally varied by less than 0.4 pH units (Fig. 1). In contrast, for flasks containing *Bacillus* sp. ± solid, pH decreased by about 1 unit and then increased and remained below the initial value of 7.4 (Fig. 1).

Bacillus sp. enhanced the release of Fe from both hornblende and goethite, with goethite showing a greater rate enhancement (Fig. 2, Table 3). Fe release rates from hornblende generally increased with increasing affinity of ligand for ferric iron, as observed by Brantley et al. (2001b) (Table 4, Fig. 3). Direct comparison of release rates between this work and Brantley et al. (2001b) cannot be made because of small differences in the preparation of the hornblende powder. Experiments which were agitated constantly released significantly more Fe to solution
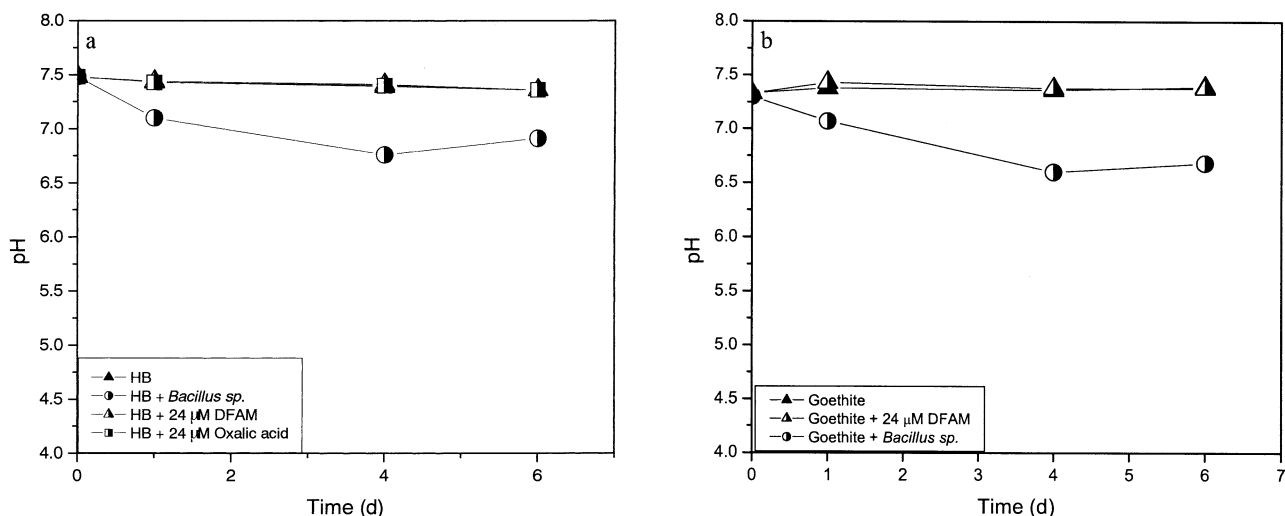
Fig. 1. Change in pH versus time in bacterial and ligand experiments with (a) hornblende (HB) or (b) goethite. Symbols represent averages over replicates as described in text.

than nonagitated experiments (Tables 3 and 4). The Fe release rate from goethite was also enhanced markedly by the presence of the siderophore DFAM (Fig. 2, Table 4).

Ferrozine assays for the experiment with hornblende (± bacteria, ± ligands) showed small concentrations of Fe^{2+} (0.28–0.5 μM) at day 1 under all conditions except where DFAM was present (Fig. 4, Table 3).

Ferrozine assays for the goethite experiments revealed that ferrous iron, if present, was beneath detection (<0.18 μM) in MM9 + goethite ± DFAM at day 4 and 6 (Table 3); however, in *Bacillus* + goethite, ferrous iron reached concentrations of approximately 1.3 μM at day 6 (Fig. 4, Table 3).

3.2. Isotopic Signature of Starting Materials

Two different batches of crushed hornblende crystal, both collected at the same time from anorthositic gneiss at Gore Mountain NY, were used here and by Brantley et al. (2001b). $\delta^{56}Fe$ values determined for these two batches were identical within $\pm 2\sigma$ (Table 3), but differ at the 1σ level of precision: 0.17 ± 0.15‰ (by Plasma54 MC-ICP-MS) for this study and −0.16 ± 0.10‰ (by TIMS) for Brantley et al. (2001b) (Table 3). This difference is outside the range of $\delta^{56}Fe$ values reported by Beard et al. (2003) for igneous rocks (±0.1‰, 2σ). However, differences in Fe isotope composition of up to ~0.5‰ between coexisting igneous minerals have also been reported Zhu et al. (2002). Therefore, subper-mil isotopic variations in high temperature geological materials are possible: $\delta^{56}Fe$ in these hornblende batches could differ by ~0.33‰. Furthermore, the samples were digested slightly differently in each case, in different laboratories. The hornblende powder used by Brantley et al. (2001b) was digested in warm HCl-HNO_3. After evaporating the HCl/HNO_3 mixture, the sample was allowed to

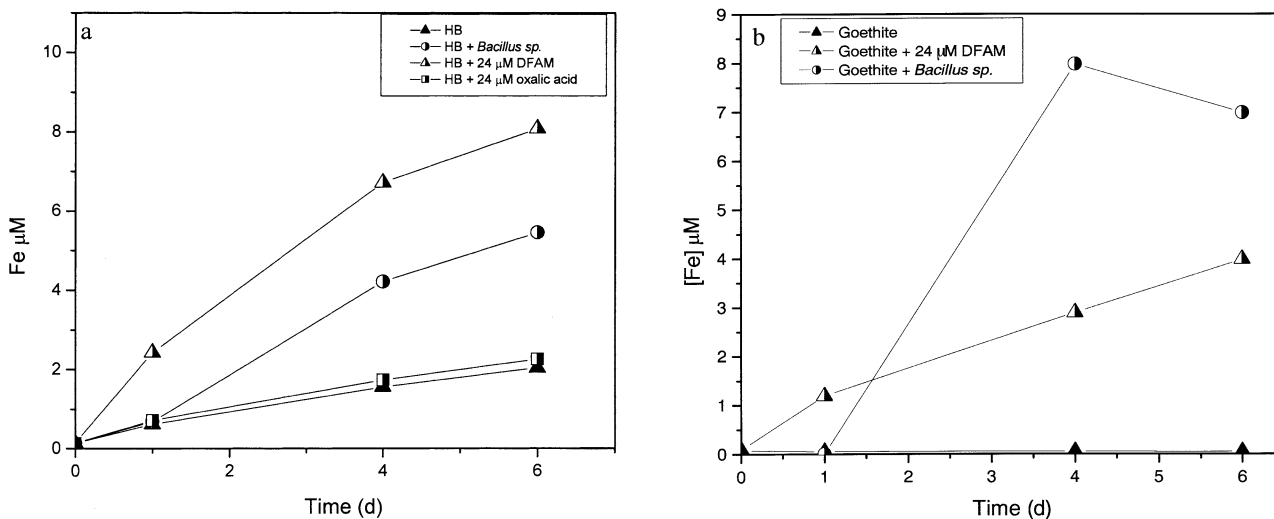

Fig. 2. Total dissolved Fe released to solution (after filtration to 0.2 μm) vs. time in bacterial and ligand experiments with (a) hornblende (HB) and (b) goethite. Symbols represent averages over replicates as described in text.

Table 3. Fe speciation and isotopic data for flask experiments.

Sample	[Fe] (μM)* 4 day	[Fe] (μM)* 6 day	[Fe^{2+}] (μM)* 4 day	[Fe^{2+}] (μM)* 6 day	[Fe^{3+}] (μM)* 4 day	[Fe^{3+}] (μM)* 6 day	δ^{56}Fe in solution‡ TIMS† (4 or 6 d as indicated)	δ^{56}Fe in solution‡ MC-ICP-MS†† (avg, 6 d)	δ^{56}Fe in solid TIMS†	δ^{56}Fe in solid MC-ICP-MS††
Hornblende[a]										0.17(3) ± 0.15
Hornblende[b]									−0.16(2) ± 0.1	
MM9 + hbl[a]	1.65	2.27						0.33(3) ± 0.15		
MM9 + hbl[a]	1.56	2.04	0.2	0.2	1.45	1.83				
MM9 + hbl[b]	3.81						−0.23(2) ± 0.15			
MM9 + hbl[b]		5.59					−0.30(2) ± 0.15			
MM9 + hbl[b]		5.41					−0.16(2) ± 0.15			
Acetic acid + hbl[a]	1.77	2.24						−0.04(3) ± 0.15		
Acetic + hbl[a] agitated		7.06						−0.90(3) ± 0.15		
Acetic + hbl[a] agitated	7.06	6.94						−0.68(3) ± 0.15		
Oxalic Acid + hbl[b]	3.76						−0.38(2) ± 0.15			
Oxalic Acid + hbl[b]		4.48					−0.40(2) + 0.15			
Oxalic Acid + hbl[b]		5.30					−0.45(2) ± 0.15			
Oxalic Acid + hbl[a]	1.73	2.26	bd	0.4	1.73	1.88				
Citric Acid + hbl[a]	2.15	2.70						−0.23(3) ± 0.15		
Citric + hbl[a] agitated	7.89	8.67						−1.01(3) ± 0.15		
Citric + hbl[a] agitated	8.19	8.67						−1.08(3) ± 0.15		
DFAM + hbl	8.36						−0.79(2) ± 0.15			
DFAM + hbl		9.78					−0.49(2) ± 0.15			
DFAM + hbl		11.67					−0.29(2) ± 0.15			
DFAM + hbl[a]	6.71	8.07	bd	bd	6.71	8.07				
Streptomyces + hbl[b]	13.91						−0.89(2) ± 0.15			
Streptomyces + hbl[b]		21.31					−0.70(2) ± 0.15			
Streptomyces + hbl[b]		23.19					−0.32(2) ± 0.15			
Bacillus + hbl[b]	29.01						−0.64(2) ± 0.15			
Bacillus + hbl[b]		44.41					−1.00(2) ± 0.15			
Bacillus + hbl[b]		35.45					−0.62(2) ± 0.15			
Bacillus + hbl[b]		49.42					−0.62(2) ± 0.15			
Bacillus + hbl[a]	4.21	5.45	0.2	0.2	3.99	5.29				
Goethite[c]										*−0.23(10) ± 0.05*
MM9 + goethite[c]	0.049	0.046	bd	bd						
DFAM + goethite[c]	2.95	3.88	bd	bd	2.95	3.88		0.11(2) ± 0.15		
DFAM + goethite[c]	2.85	3.98	bd	bd	2.85	3.98		−0.14(2) ± 0.15		
DFAM + goethite[c]	2.87	4.09	bd	bd	2.87	4.09		−0.04(1) ± 0.15		
Bacillus sp. + goethite[c]	4.10	5.06								
Bacillus sp. + goethite[c]	8.34	6.20	1.51	1.05	6.83	5.15		*−1.51(1) ± 0.05*		
Bacillus sp. + goethite[c]	7.88	6.74	1.28	1.17	6.60	5.57		*−1.68(3) ± 0.05*		
Bacillus sp. + goethite[c]	7.73	8.22		1.51		6.71		*−1.82(3) ± 0.05*		

δ^{56}Fe data are reported relative to the IRMM standard, ~ 0.09‰ lighter than the BIR standard used in Brantley et al. (2001 b) and Bullen et al. (2001)

* Dissolved total Fe, Fe^{2+}, or Fe^{3+} concentration in filtered solution after 4 or 6 days.

bd = beneath detection, which for ferrous iron determination is estimated at ≤0.18 μM. Blank spaces indicate no analysis was made.

† TIMS data from Brantley et al. (2001b).

†† MC-ICP-MS data were obtained using the VG Plasma54 (1σ external precision ~ ±0.15‰), except for data in italics which were obtained using the Finnigan Neptune (1σ = ±0.05‰). Reported values are the means of two or more replicate analyses of each sample.

‡ δ^{56}Fe data from this work and from Brantley et al. (2001). For one of the *Streptomyces* experiments, little cell growth occurred and one data point was not included in average (as described in Brantley et al., 2001b). Number in parentheses indicates number of replicate isotopic measurements. All replicates agreed within stated external precision. Means of replicates are reported.

[a] Hornblende (hbl) starting material isolated from Gore Mtn. anorthositic gneiss. 0.19 m^2/g specific surface area; ratio of surface area to volume of experiment = 6.33.

[b] Hornblende from same locality as above, but picked as a different separate and ground separately to 0.17 m^2/g.

[c] Goethite starting material with 30.6 m^2/g specific surface area, dissolved completely with citrate-dithionite method for 25 h.

sit in 6 N HCl for several days under heat. In that state, a small aliquot of the 6 N HCl solution (the appropriate amount of liquid to yield 1.25 μg of Fe) was combined with added Fe for the double spike for analysis in the thermal ionization mass spectrometer. For the data reported here, hornblende powder was dissolved using a microwave-assisted acid digestion designed for siliceous matrices (Kingston and Walter, 1995).

Samples were evaporated to remove HF, and then resuspended in 2% nitric acid. In both cases, samples were processed through chromatography to extract Fe for mass spectrometric analyses.

To analyze the goethite, 0.006 g of synthetic goethite was combined with 25 mL of 0.68 mol/L sodium citrate and 0.4 g of sodium dithionite and shaken for 25 h. At the end of 25 h no

Table 4. Metal Release Rates.

Solid	Specific surface area (m²/g)	Condition	SA/vol[a] (m²/L)	Fe[b] (mol · m⁻² · s⁻¹) × 10⁻¹³
Goethite	30.6	MM9	306	bd
Goethite	30.6	*Bacillus* sp.	306	1.0 ± 0
Goethite	30.6	DFAM	306	0.195 ± 0.007
Hornblende	0.19	MM9	6.33	5.1 ± 0.5
Hornblende	0.19	*Bacillus* sp.	6.33	17 ± 3
Hornblende	0.19	Acetic acid	6.33	4.3 ± 0.8
Hornblende	0.19	Acetic acid agitated	6.33	7.1 ± 1.3
Hornblende	0.19	Citric acid	6.33	6.4 ± 0.4
Hornblende	0.19	Citric acid agitated	6.33	8.8 ± 3.0
Hornblende	0.19	Oxalic acid	6.33	5.5 ± 0.5
Hornblende	0.19	DFAM	6.33	20 ± 4

[a] Total surface area of solid/volume of MM9 used.

[b] Linear release rates calculated for the first several days of dissolution (not including concentrations at t = 0). For the goethite + *Bacillus* experiment, release rate was calculated after the induction period.

visible solid remained and analysis of the final solution confirmed that all of the goethite solid had dissolved. The isotopic composition of the goethite, measured by MC-ICP-MS on this digested sample, is ~ -0.23 ± 0.1 (2σ; Neptune MC-ICP-MS)‰ (Table 3).

3.3. Isotopic Measurement of Aqueous Fe

For this study, it is most useful to consider the offset in $\delta^{56}Fe$ between starting materials and products (e.g., see Table 5: $\Delta^{56}Fe = \delta^{56}Fe_{solution} - \delta^{56}Fe_{hornblende}$) rather than the absolute values of $\delta^{56}Fe$ (Table 3). For example, Fe dissolved from hornblende in the presence of citric acid is lighter than Fe in the bulk hornblende by -0.40 ± 0.21‰. In contrast, Fe in solution with MM9 without organic ligands is indistinguishable from Fe in the mineral. Fe dissolved in the presence of acetic acid is insignificantly fractionated ($\Delta^{56}Fe = -0.13 \pm 0.21$‰).

The direction of fractionation is consistent with the observations of Brantley et al. (2001b). In all hornblende experiments with strong organic ligands, the isotopic composition of solution is lighter than the starting mineral. When data from

this and the earlier study are combined, a correlation is observed between $\Delta^{56}Fe$ and log K_{assoc} for acetic acid, oxalic acid, citric acid and DFAM (Fig. 5). Much larger effects were observed in the constant agitation experiments with acetic and citric acids: $\Delta^{56}Fe = -1.0$ and -1.2‰, respectively. Again $\Delta^{56}Fe$ is larger for the ligand with the higher value of log K_{assoc}.

Little or no fractionation was observed in this study between dissolved Fe and goethite in the abiotic DFAM experiments (Table 5). However, Fe released from goethite + *Bacillus* was much lighter than Fe in the goethite starting material: $\Delta^{56}Fe = -1.44 \pm 0.16$‰. This is a larger fractionation than observed in either biotic or abiotic hornblende experiments (Table 5).

3.4. Soil Extractions

The citrate-dithionite procedure used for Fe oxides (Hendershot et al., 1993) was chosen because it is reported to remove
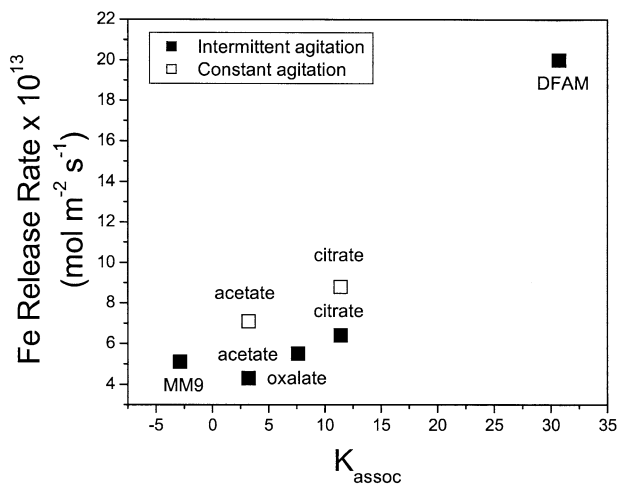

Fig. 3. Dissolved Fe release rate (Table 4) from hornblende in ligand experiments plotted vs. log K_{assoc} value for ligand (Table 2).
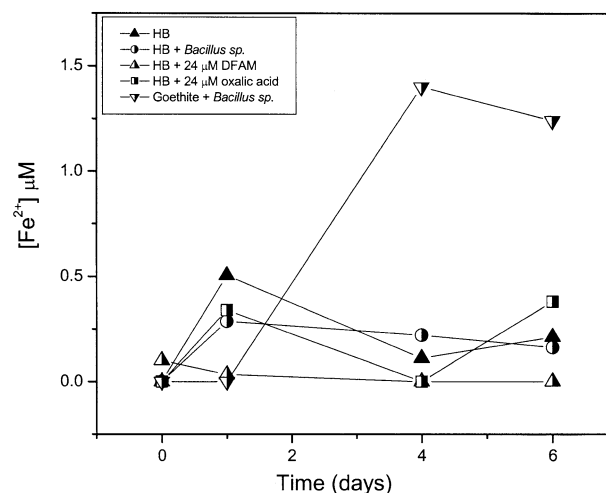

Fig. 4. [Fe^{2+}] vs. time in filtered solutions from mineral ± bacteria ± organic ligands (oxalic acid, DFAM) experiments. [Fe^{2+}] was determined by the ferrozine assay. Data summarized in Table 3. Detection limits estimated at 0.18 μM. In some cases symbols are plotted beneath detection.

Table 5. $\Delta^{56}Fe = \delta^{56}Fe_{solution} - \delta^{56}Fe_{starting\ material}$.[a]

Sample	Day measured	$\Delta^{56}Fe$	Reference
DFAM—goethite	6	0.34 ± 0.16	This work
	6	0.09 ± 0.16	
	6	0.19 ± 0.16	
		0.21 ± 0.16	average
Bacillus culture—goethite	6	−1.28 ± 0.07	This work
	6	−1.45 ± 0.07	
	6	−1.59 ± 0.07	
		−1.44 ± 0.16	average
MM9—hornblende	4	−0.07 ± 0.18	Brantley et al. (2001b)
	6	−0.14 ± 0.18	
	6	0.00 ± 0.18	
		−0.07 ± 0.18	average
MM9—hornblende	6	0.16 ± 0.21	This work
Acetic—hornblende	6	−0.13 ± 0.21	This work
Acetic—hornblende agitated	6	−1.07 ± 0.21	This work
Acetic—hornblende agitated	6	−0.85 ± 0.21	
		−0.96 ± 0.21	average
Oxalic—hornblende	4	−0.22 ± 0.18	Brantley et al. (2001b)
	6	−0.24 ± 0.18	
	6	−0.29 ± 0.18	
		−0.25 ± 0.18	average
Citric—hornblende	6	−0.40 ± 0.21	This work
Citric-hornblende agitated	6	−1.18 ± 0.21	This work
Citric-hornblende agitated	6	−1.25 ± 0.21	
		−1.22 ± 0.21	average
DFAM—hornblende	4	−0.63 ± 0.18	Brantley et al. (2001b)
	6	−0.33 ± 0.18	
	6	−0.13 ± 0.18	
		−0.36 ± 0.25	
Bacillus culture—hornblende	4	−0.48 ± 0.18	Brantley et al. (2001b)
	6	−0.84 ± 0.18	
	6	−0.46 ± 0.18	
	6	−0.46 ± 0.18	
		−0.56 ± 0.19	average
Streptomyces culture—hornblende	4	−0.73 ± 0.18	Brantley et al. (2001b)
	6	−0.54 ± 0.18	
	6	−0.16 ± 0.18	
		−0.48 ± 0.29	average

[a] Error in $\Delta^{56}Fe$ represents either the propagated error from isotopic measurements for solution and solid, or standard deviation of multiple measurements, whichever is greater.

both amorphous and crystalline Fe oxides without dissolving silicate minerals (Mehra and Jackson, 1960). Complete removal of Fe oxides by this method was verified in two ways. The soil that remained after the first extraction was rinsed with distilled-deionized water and treated with the citrate-dithionite solution for 17 h a second time. The second extraction contained less than 3% as much Fe as the first extraction, indicating that the first extraction had dissolved virtually all of the available Fe oxide in the samples.

The soil extraction samples (both exchangeable and oxide samples) were also analyzed for Fe, Al, and Si. The exchangeable fraction of the soil contained approximately 10.0 μg Fe per gram of soil, 334 μg Al per gram of soil, and 5 μg Si per gram of soil. The oxide extraction of the soil yielded 7700 μg per gram of soil Fe, 1600 μg per gram of soil Al, and 282 μg per gram of soil Si. The low levels of Si compared to Fe and Al in these extractions indicate that silicates are not dissolving during either extraction. The Al in the oxide extraction presumably derives from Al substituted for Fe in the oxide minerals.

Isotopic analysis of the soil extractions shows that Fe on the

cation exchange complex has a $\delta^{56}Fe$ value of −1.33‰, while $\delta^{56}Fe$ in oxides is −0.20‰ (data for Soil 2 in Table 6). The difference between the exchangeable and oxide fractions is similar within error to that reported by Brantley et al. (2001b) for a different soil horizon from the same site (Soil 1 in Table 6); however, the magnitudes of the $\delta^{56}Fe$ values for extractant solutions differ for the two soil samples.

The low levels of Si present in both the exchangeable and oxide extraction solutions indicate that neither of the extraction procedures causes congruent dissolution of silicate minerals. Therefore, the $\delta^{56}Fe$ values of the extracted Fe should reflect the isotopic composition of the exchangeable reservoir, and not the silicate minerals, such as hornblende, in the soil. Incomplete extraction procedures could fractionate Fe, however. To test for fractionation during extraction, Fe isotopes were measured on a citrate-dithionite extractant solution reacted with goethite for 2 h: 0.006 g of synthetic goethite (synthesized in the same batch as described previously) was combined with 25 mL of sodium citrate and 0.4 g of sodium dithionite and the mixture was shaken and a 4 mL sample was collected at 2 h. The lack of isotopic difference between the citrate-dithionite solution ob-
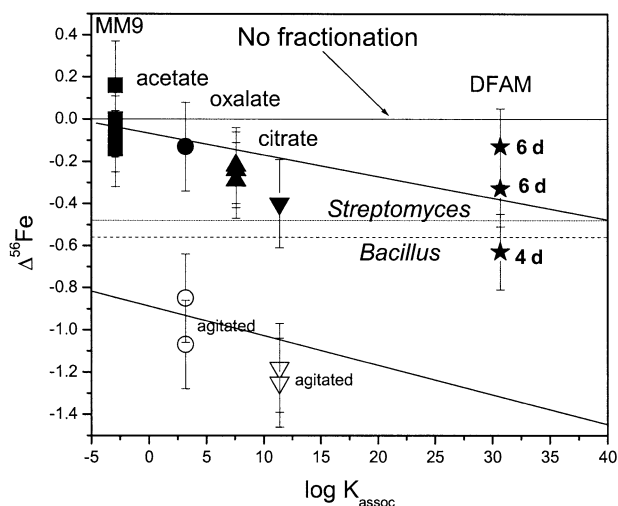
Fig. 5. $\Delta^{56}\text{Fe}$ ($\delta^{56}\text{Fe}_{\text{solution}} - \delta^{56}\text{Fe}_{\text{hornblende}}$) for hornblende dissolution experiments in the presence of the noted ligands or in MM9 medium plotted vs. log K_{assoc}, the association constant from Table 2. Horizontal lines indicate values of $\Delta^{56}\text{Fe}$ for bacteria experiments from Brantley et al. (2001b). In these experiments, both bacteria (*Streptomyces* sp., *Bacillus* sp.) are known to produce catecholate siderophores, which are reported to have higher association constants than hydroxamate siderophores such as DFAM; however, K_{assoc} is unknown for siderophores in these experiments. Horizontal solid line marked "No fractionation" indicates expected isotopic value for Fe released when identical to hornblende starting material. Data summarized in Table 5. Experiments that were intermittently (solid symbols) and constantly agitated (open symbols) are plotted for acetate and citrate. Days at which the samples were taken is indicated for just the DFAM experiment.

tained after 2 (incomplete dissolution) and 25 h (complete dissolution) from synthetic goethite (Tables 3 and 6) documents that citrate-dithionite does not fractionate Fe measurably during extraction. Therefore, the isotopic signature of Fe oxyhydroxides in the Gore Mountain soil (citrate-dithionite extracted) is identical ($\pm 2\sigma$) to the hornblende in that soil for both Soil 1 and Soil 2 (Table 6).

To test for fractionation during extraction of labile Fe, we

tried the MgCl_2 extraction on a new sample of Gore Mountain soil (Soil 2, sample 2) for 1 h and 20 h instead of the original 2 h, and observed that our measured value for the 1 h and 20 h analyses for sample 2 (-2.65 and $-2.86‰$) were identical to each other within error. The values did differ substantially, however, from that measured for the 2 h extraction on sample 1 of Soil 2 ($-1.33‰$, Table 6). The similarity between the measured values at 1 and 20 h documents that the extraction procedure does not cause fractionation; however, significant differences between exchangeable Fe measured on different soils are consistent with isotopic variability within this labile fraction.

4. DISCUSSION

4.1. Siderophores and Dissolution

Fe release from hornblende crystal is accelerated in the presence of *Bacillus* sp. due to release of low molecular weight organic acids such as oxalic acid, and especially to the release of a catecholate siderophore (Kalinowski et al., 2000a,b; Liermann et al., 2000a; Brantley et al., 2001b). In abiotic experiments, Fe release rates from hornblende crystal increase with the concentration of the commercially available siderophore, DFAM (Liermann et al., 2000a), consistent with the hypothesis that dissolved siderophore forms surfaces complexes with Fe at the mineral surface, weakening the bonds between Fe and the mineral lattice (Kalinowski et al., 2000a). Such bond weakening is thought to enhance Fe-ligand complex release to solution. Enhanced release of Fe to solution in the presence of bacteria and organic ligands is consistent with Fe-depletion of a surface layer on hornblende, which has also been documented for glass and crystal with X-ray photoelectron spectroscopy (XPS, Kalinowski et al., 2000a).

A new observation from this study is consistent with the hypothesis that siderophores promote dissolution of Fe oxides. Production of siderophores is repressed when bacteria are grown under Fe-replete conditions such as that used here for growth before inoculation into experimental flasks. After inoculation into Fe-depleted MM9, Fe release from goethite was not

Table 6. Fe isotopic data for soil and goethite extractions.

Sample	Solid extracted	Duration of extraction	$\delta^{56}\text{Fe}$ in extractant	
			TIMS[†]	MC-ICP-MS[††]
Hornblende			$-0.16\,(2) \pm 0.1$	
Hornblende				$0.17\,(3) \pm 0.15$
Citrate-dithionite	Soil 1	17 h	$0.25\,(2) \pm 0.15$	
Citrate-dithionite	Soil 2, sample 1	17 h		$-0.20\,(1) \pm 0.15$
Citrate-dithionite	Goethite	2 h		$-0.15\,(5) \pm 0.15$
Citrate-dithionite	Goethite	25 h		*$-0.23\,(5) \pm 0.05$*
Citrate-dithionite	Goethite	25 h		*$-0.22\,(5) \pm 0.05$*
Exchangeable	Soil 1	2 h	$-0.76\,(2) \pm 0.15$	
Exchangeable	Soil 2, sample 1	2 h		$-1.33\,(3) \pm 0.15$
Exchangeable	Soil 2, sample 2	1 h		$-2.65\,(2) \pm 0.15$
Exchangeable	Soil 2, sample 2	20 h		$-2.86\,(3) \pm 0.15$

[†] TIMS data from Brantley et al. (2001b).
[††] MC-ICP-MS data were obtained using the VG Plasma54 (1σ external precision $\sim \pm 0.15‰$), except for data in italics which were obtained using the Finnigan Neptune ($1\sigma \sim \pm 0.05‰$). Reported values are the means of replicate analyses of each sample where number of replicates are given in parentheses.

significant during the first 1 d (Fig. 2), during which period siderophore production was presumably stimulated (induction period). No evidence for an induction period is observed in the hornblende experiments where Fe release occurs abiotically even before siderophore concentrations are significant in solution, nor in the organic ligand experiments (Fig. 2).

4.2. Fe Redox Chemistry

The MM9 medium was measured by ICP-MS to contain 60 $\pm$ 8 nM Fe but this low value lies close to or below the detection limits of our instrument for Fe. This value is approximately 30 times higher than values calculated to be in equilibrium with goethite at pH 7.39 in MM9 solution (2 nM) as calculated by Geochemists Workbench, v. 4.0 (NIST, 1998; Bethke, 2002) using an updated version of the thermodynamic database of Delany and Lundeen (1991) with added constants from NIST (1998). Complexation reactions with casamino acids, glucose, and other organic compounds for which complexation constants are unavailable were not included in this calculation. After abiotic reaction with goethite for 6 d, Fe concentrations in solution were measured at 46 $\pm$ 6 nM (Table 3). Indistinguishable values of dissolved Fe (albeit both at the level of the detection limits) in MM9 before and after reaction with goethite are consistent with insignificant or at least unmeasurable dissolution of goethite in abiotic MM9.

In contrast to abiotic dissolution, dissolution of goethite in the presence of bacteria yielded measurable ferrous and ferric iron in solution after several days (Figs. 2 and 4). The production of Fe^{2+} in solution in goethite + bacteria flasks is consistent with the fact that flasks were only intermittently stirred, allowing the oxygen concentration to drop as bacteria grew. In the presence of low redox potential, goethite can dissolve reductively, and such reductive dissolution can be enhanced by organic ligand complexation. Fe^{2+} in solution can also act as a reductant for Fe oxides, either with or without organic ligands, when thermodynamically favorable (Stumm and Sulzberger, 1992). Reduction of Fe^{3+} by some siderophores in solution is also possible (Hider, 1984), and Suter et al. (1988) have shown that a complex-forming ligand alone can accelerate dissolution of Fe oxide, but the presence of ferrous iron in solution along with the ligand (i.e., a reductant and a complex former) can accelerate dissolution further.
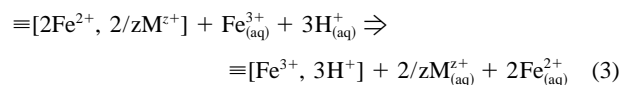
Both Fe^{2+} and Fe^{3+} were also observed in solution with hornblende after several days under abiotic and biotic conditions (Table 3, Figs. 2 and 4). Our observations of ferrous iron released from hornblende under aerobic conditions are consistent with observations by White and Yee (1985), who observed Fe^{2+} in solution during dissolution of hornblende in abiotic oxygenated solutions at neutral pH. Despite the presence of Fe^{2+} in solution, they observed the mineral surface to be dominated by Fe^{3+} as measured by XPS in the same experiments.

To explain the observation of ferrous iron in solution in flasks with a mineral dominated by ferric iron at the surface, we note that hornblende crystal contains ferric and ferrous ions and acts as a source of electrons to a solution: the Fe^{2+}/Fe^{3+} ratio in Gore Mountain hornblende measured on similar crystal from the same locality is 3.6 (Liermann et al., 2000b). Hydrolysis of

surface Fe^{3+}, $\equiv Fe^{3+}$, and release to solution can be expressed as

$$\equiv Fe^{3+} + 3H_2O \Rightarrow \equiv H_3^{3+} + Fe^{3+}_{(aq)} + 3OH^-_{(aq)} \quad (2)$$
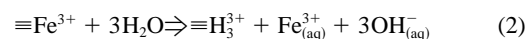
White and Yee (1985) point out that Fe^{3+} in solution will oxidize Fe^{2+} at the hornblende surface, $\equiv Fe^{2+}$, releasing surface cations of charge z, $\equiv M^{z+}$, to solution:

$$\equiv [2Fe^{2+}, 2/zM^{z+}] + Fe^{3+}_{(aq)} + 3H^+_{(aq)} \Rightarrow$$
$$\equiv [Fe^{3+}, 3H^+] + 2/zM^{z+}_{(aq)} + 2Fe^{2+}_{(aq)} \quad (3)$$

Oxidation of surface Fe can also occur through interaction with dissolved oxygen:

$$\equiv [Fe^{2+}, 1/zM^{z+}] + 1/4O_2 + H^+_{(aq)} \Rightarrow$$
$$\equiv Fe^{3+} + 1/zM^{z+}_{(aq)} + 1/2H_2O \quad (4)$$
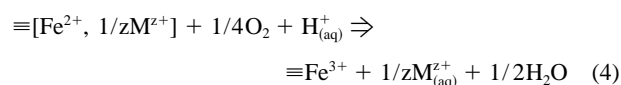
wherein pO_2 is drawn down. Oxidation of Fe is hypothesized to occur to depths of $\sim$60 Angstroms in the hornblende crystal during open system dissolution over 24 h and to be rate-controlled by cation diffusion through the leached layer (White and Yee, 1985). For example, in experiments not reported here, we have observed layers as deep as 250 Angstroms to be Ca or Mg deficient compared to bulk crystal when hornblende was dissolved at pH 5.6 in $HCl-H_2O$ solutions for 9000 h (unpublished data). Such deep layers may represent cation leaching of Ca or Mg at the mineral surface. Oxidation of ferrous ions in the hornblende surface (Eqns. 3 and 4), release of Fe^{3+} to solution (Eqn. 2), and incomplete reduction of ferric to ferrous ions in solution (Eqn. 3) explains the presence of both Fe^{2+} and Fe^{3+} in solution during hornblende dissolution (Table 3, Fig. 4).

4.3. Fe Isotope Fractionation

4.3.1. Abiotic hornblende experiments

To explain Fe isotope fractionation during hornblende weathering we must explain: i) Preferential accumulation of lighter vs. heavier Fe isotopes in solution (Tables 3 and 5); ii) Increased magnitude of fractionation in continuously agitated abiotic experiments (Tables 3 and 5; Fig. 5); iii) The apparent correlation between $\Delta^{56}Fe$ and log (K_{assoc}) (Fig. 5).

Observation (i) is consistent with a simple kinetic isotope effect during dissolution. However, this is not a unique interpretation and so other constraints are needed. Observation (ii) suggests that the isotope effect is related to interactions at the mineral surface, since agitation enhances the extent of interaction of fresh mineral surfaces with reactive solution. Without agitation, high concentrations of dissolved cations develop at the mineral-water interface and net dissolution ceases. Agitation may also cause particle abrasion, exposing fresh surface Fe to solution. Three types of mechanisms are potentially consistent with these observations: a. Incongruent dissolution of isotopically distinct Fe-bearing secondary phases or zones in the bulk solid phase; b. Precipitation of heavy Fe-enriched secondary phases, or preferential adsorption of heavy Fe, onto mineral surfaces; c. Preferential release of light Fe during development of a "leached layer" on the surface of an isotopically homogenous bulk solid.

Each of these possibilities is considered in detail below. Special attention is paid to consistency with observation (iii).

4.3.1.1. Incongruent dissolution of bulk mineral. Incongruent dissolution of isotopically distinct Fe-bearing reservoirs must be considered because hornblende contains both Fe^{2+} and Fe^{3+} and dissolves nonstoichiometrically (Brantley and Chen, 1995). Isotopically distinct reservoirs could include isotopic "zones" within the mineral (Skulan et al., 2002) or impurity phases.

The first of these possibilities is easily dismissed because powdered hornblende was used in these experiments. This should homogenize any isotopic zonation which might have developed during mineral growth.

Isotopic contributions from impurities are not so easily dismissed, because this mineral is known to contain chlorite and other impurities (Liermann et al., 2000b). Additionally, the rate at which Fe-chelating ligands preferentially dissolve impurities could correlate with equilibrium binding constants (observation (iii)).

However, Fe isotopic fractionation between igneous or metamorphic minerals is likely small because Fe in such systems is presumably at isotopic equilibrium and the magnitude of equilibrium fractionation factors decreases with increasing temperature (Urey, 1947; Schauble et al., 2001). Measurements support this prediction. For example, Beard et al. (2003) reported no variation in $\delta^{56}Fe$ among terrestrial and lunar basalts to within ± 0.1‰ (2σ). Sharma et al. (2001) reported variations of ~ 0.5‰ between Fe in terrestrial basalts and deep-sea hydrothermal fluids, but these fluids lost Fe at temperatures as low as $\sim 350°C$, substantially lower then the $\sim 600°C$ temperatures likely experienced during formation of the anorthositic gneiss from which the hornblendes in this study were obtained. Zhu et al. (2002) have reported Fe isotope fractionations equivalent to $\delta^{56}Fe$ offsets of $< \sim 0.3$‰ between coexisting olivines and pyroxenes in mantle xenoliths, and between olivine and Fe metal in pallasite meteorites. The largest effect they report is ~ 0.5‰ between coexisting olivine and amphibole in a mantle xenolith.

Because the bulk hornblende is also dissolving in our experiments, the postulated isotopic offset between the bulk mineral and the preferentially dissolved impurities would have to be $\geqslant 0.5$‰ to explain the data in Table 5. For example, if 10% of the Fe in solution after 6 d were from impurity phases and if the isotopic composition of these impurities was 0.5‰ lighter than the bulk mineral, then the isotopic offset between dissolved and bulk Fe would be only ~ 0.05‰.

A final possibility of this type is isotope fractionation between Fe^{2+} and Fe^{3+} in the mineral. The bonding environments for these oxidation states in hornblende can differ, as required to drive equilibrium isotope fractionation (Urey, 1947; Schauble et al., 2001). The apical oxygens of two silicate tetrahedra in chain silicates are octahedrally coordinated by small cations such as Mg or Fe (*M1, M2* and *M3* sites in amphiboles). Larger cations such as Ca usually occupy the sites formed by opposed tetrahedral bases where coordination is irregular (the *M4* site). However, considerable variation exists, and Ca, Na, Mg, or Fe^{2+} are often found in the *M4* site while Mg, Fe^{2+}, Fe^{3+}, or Al can be commonly found in the *M1, M2*, and *M3* sites. Differences in bonding environment for some of the ferrous and ferric ions are thus expected in hornblende.

However, as with intermineral variations, the magnitude of such differences in igneous and metamorphic minerals is likely to be smaller than required to account for the observations.

4.3.1.2. Precipitation/adsorption. Separation of dissolved Fe species that are in isotopic equilibrium in solution can give rise to substantial isotope effects (e.g., Bullen et al., 2001; Johnson et al., 2002; Roe et al., 2003), shifting the isotopic composition of the dissolved pool. Kinetic isotope effects may also fractionate Fe isotopes during species separation.

In our hornblende systems, the most significant dissolved species are likely Fe^{2+} and Fe^{3+} aquo complexes and Fe^{3+}-organic complexes. Isotope fractionation of 1–5‰ between dissolved Fe^{2+} and Fe^{3+} complexes seems likely (Schauble et al., 2001; Johnson et al., 2002). Fractionation will favor concentration of the heavier isotopes in Fe^{3+} complexes, due to the stronger bonding environment. Two separation processes seem most probable: precipitation or adsorption.

Very small amounts of a white powder were observed to precipitate from MM9 medium within 24 h after addition of $CaCl_2$. To assess precipitation in the medium, MM9 media was prepared and filtered (0.2 μm) after 24 h. Although not enough precipitate could be collected for X-ray diffraction, analysis by Energy Dispersive Spectroscopy on the SEM documented that it contained P, Cl, Ca, Na, O, and C. The precipitate is therefore most probably a Ca phosphate. Consistent with these observations, we calculated speciation in MM9 $\pm$ organic ligands, using Geochemists Workbench (Bethke, 2002) and organic-Fe complexation constants from NIST (1998) and determined that hydroxyapatite is supersaturated in the starting medium. These calculations were also completed for solutions analyzed from experiments. For all measured concentrations in hornblende experiments with MM9, acetic acid, oxalic acid or citric acid, the calculations show that one or more of the following Fe-containing phases were also supersaturated during our experiments: nontronite, hematite, magnetite, strengite, goethite, as well as Fe-containing amorphous phases. All experiments with hornblende were also supersaturated with respect to diaspore.

If an Fe-containing precipitate forms in the experiments, an active $Fe(OH)_3$ amorphous precipitate (Langmuir and Whittemore, 1971), or an Fe $\pm$ Al $\pm$ P amorphous precipitate is most likely, given the saturation indices and the ease of precipitation of such phases. Because we calculated equilibria for filtered solutions, however, if precipitation had occurred, particulates must have been small enough to pass a 0.2 μm filter. Such Fe particles may have been present: for example, Langmuir and Whittemore (1971) showed that ferric oxyhydroxides with crystal dimension on the order of 10 nm can remain in solution indefinitely in some natural waters. However, such small precipitates could not explain the isotopic fractionation observed since they remained suspended in solution after filtration.

Formation of ferric oxide precipitates of grain size greater than 0.2 μm, if it occurs, is expected to drive the residual dissolved Fe pool to lighter values as observed, because dissolved ferric iron is expected to be isotopically heavy compared to ferrous iron (Schauble et al., 2001; Johnson et al., 2002). Increased interaction of surface area of solid phases with solution in the agitated experiments might lead to more effective removal of precipitate particles from solution, leading to more fractionation as observed in agitated experiments.

Significantly, however, calculations indicate that all Fe-con-

taining phases were *undersaturated* in the experiments with DFAM; no precipitation of an Fe phase is expected in this system. If isotopic fractionation was controlled by precipitate formation, therefore, we would have expected to see no fractionation at all in the experiment with DFAM. Yet, Fe released from hornblende dissolved with DFAM after 4 d showed one of the largest isotopic fractionation of the unagitated ligand experiments (Tables 3 and 5, Brantley et al., 2001b). Furthermore, we would have predicted *more* precipitation (and hence *more* fractionation of the dissolved pool) in the presence of ligands of lower affinity for Fe. This is the opposite trend from that which was observed (Fig. 5). Thus, while precipitation may contribute to fractionation in hornblende systems, it does not appear to be the primary control.

Unlike precipitation, adsorptive loss of Fe^{2+} from solution probably occurred in *all* hornblende experiments. It is well known that adsorption of Fe^{2+} onto bacterial surfaces and onto mineral powders can occur (LaKind and Stone, 1989; Liu et al., 2001; Icopini et al., 2004); therefore, adsorption would be expected in all experiments where $Fe^{2+}_{(aq)}$ is present. In contrast, aquo complexes of Fe^{3+} in solution at circum-neutral pH are expected to undergo hydrolysis and precipitate as amorphous phases rapidly, while we assume that Fe^{3+}-organic complexes will not adsorb to mineral surfaces extensively. Therefore, adsorption is expected to occur only for ferrous, not ferric, iron. It is not clear, however, how such an effect could account for the $\Delta^{56}Fe$ vs. log K_{assoc} correlation (Fig. 5), nor how adsorption could explain isotopic fractionation observed in the hornblende + DFAM experiment, where no Fe^{2+} was observed in solution (Table 3, Fig. 4). Difficulty in accounting for the correlation in Figure 5 also leads us to suspect that equilibrium fractionation between dissolved Fe^{2+} and ferric oxide precipitates or other solid phases is not a primary control. Furthermore, once again, no ferrous ions were measured in hornblende + DFAM experiments (Table 3), and yet fractionation was measurable for that experiment. Kinetic isotope effects during precipitation are also unable to explain the data because such processes should preferentially remove light isotopes from solution, leaving the solution heavy compared to the bulk mineral.

We conclude that equilibrium isotopic fractionation effects may occur during adsorption of ferrous iron. Precipitation as a fractionation mechanism is not required to explain our results but we cannot disprove contributions from this phenomenon. Neither adsorption nor precipitation can explain all our observations.

4.3.1.3. Preferential dissolution from a leached layer. We can consider equilibrium or kinetic isotope effects that might occur during formation of an Fe-leached layer on the hornblende surface. In principle, equilibrium isotope effects between different surface species combined with preferential dissolution of one species over others could drive fractionation. However, equilibrium fractionation between surface-bound Fe^{2+} and Fe^{3+} would be expected to concentrate heavy Fe in Fe^{3+}, as occurs in solution. Because organic Fe-chelating ligands have a much higher affinity for Fe^{3+} than Fe^{2+}, dissolution would be expected to favor transfer of heavy Fe into solution. Similarly, equilibrium between surface-bound Fe^{3+} and Fe^{3+}-$L_{(aq)}$ (where L is the organic ligand) would be expected to favor partitioning of heavy Fe into the stronger

bonding environment of the organic chelate, driving the solution to isotopically heavy values as Fe^{3+}-L leaves the surface.

A kinetic isotope effect during oxidation of surface-bound Fe^{2+} or chelation of surface-bound Fe^{3+} by organic ligands was first proposed in Brantley et al. (2001b). However, it has been argued that the isotopic composition of dissolved Fe should be identical to Fe in the bulk as dissolution proceeds along a reaction front (e.g., Johnson et al., 2002). Such simple homogeneous dissolution along a reaction front does not always occur in aluminosilicates however. Rather, a "leached" layer is formed through which non–network-forming cations such as Fe must diffuse (e.g., Mogk and Locke, 1988; Brantley and Chen, 1995; Frogner and Schweda, 1998). Kalinowski et al. (2000a) reported XPS evidence for the development of Fe-depleted, Si-enriched leach layers at the surface of hornblende planchets incubated with *Bacillus* sp. Such a leached layer might be homogeneous everywhere on the mineral surface, or might be extensive at some sites, for example, at dissolution pits. No Fe-depleted layers were observed by either Kalinowski et al. (2000a) or Buss et al. (2003) on planchets (hornblende crystal or glass of hornblende composition respectively) incubated with sterile medium without ligands.

Furthermore, hornblende dissolution, like dissolution of other silicates (e.g., White and Brantley, 1995), does not reach steady state stoichiometric dissolution even after thousands of hours (Frogner and Schweda, 1998). Indeed, Mogk and Locke (1988) observed cation depletion over the upper 1200 Angstroms of altered surface of a hornblende grain weathered for more than 100,000 yr, and inferred from the extent of depletion and the profile geometry that steady state had not been attained. In our 6-d experiments, therefore, we are justified in concluding that leached layer development is ongoing, rather than at steady state. During this transient period, kinetic isotope effects can be expressed.

We illustrate this effect by a simple time-dependent model of Fe release to solution from a leached-layer. The rate of change of Fe concentration in the leached layer (C) is:

$$dC/dt = F_{in}/x - kC \qquad (5)$$

where F_{in} is the rate per unit area of Fe supplied to the leached layer at the bulk mineral-leached layer interface; x is the thickness of the leached layer; and k is a pseudo–first-order rate constant for Fe release from the layer to solution (surface reaction rate constant). For simplicity in this illustrative model, we ignore the time-dependence of x and the diffusive effects during transport through the leached layer.

The general solution to this equation is

$$C(t) = \frac{F_{in}}{kx}(1 - e^{-kt}) + C_0 e^{-kt} \qquad (6)$$

where C_0 is the Fe concentration in the mineral. Treating ^{54}Fe and ^{56}Fe as independent species, we derive,

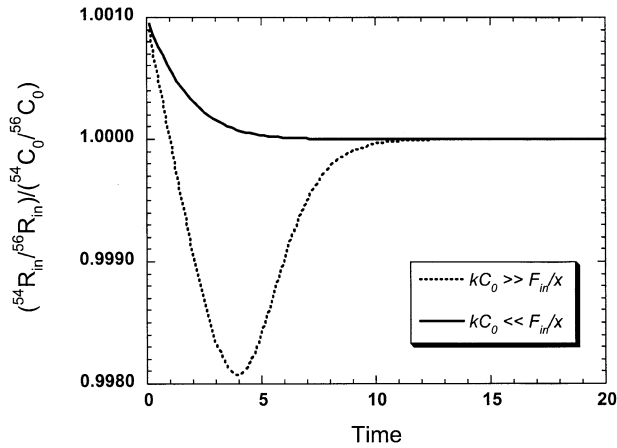$$^{54}C(t) = \frac{^{54}F_{in}}{^{54}kx}(1 - e^{-^{54}kt}) + {}^{54}C_0 e^{-^{54}kt} \qquad (7)$$

and

Fig. 6. Calculated fractionation of Fe isotopes during transfer from the leached layer to solution. For illustration, we assume $^{54}k/^{56}k = 1.0010$ initially (see text). Time units are arbitrary. The instantaneous fractionation of ^{54}Fe from ^{56}Fe leaving the leached layer (($^{54}R_{in}/^{56}R_{in}$)/($^{54}C_0/^{56}C_0$)) is initially 1.0010 (i.e., the initial Fe leaving the leached layer is 1‰ light relative to the bulk mineral) and evolves to 1.0000 (0‰; identical to the bulk mineral) as the isotopic composition of the leached layer attains a steady state in which the rate of supply of each isotope to the leached layer balance the rate of loss to solution. The trajectory of this evolution with time depends on the relative magnitudes of kC_0 and $F_{in/x}$ (see text).

$$^{56}C(t) = \frac{^{56}F_{in}}{^{56}kx}\left(1 - e^{-^{56}kt}\right) + {^{56}C_0}e^{-^{56}kt} \tag{8}$$

The rates at which ^{54}Fe and ^{56}Fe atoms enter solution are $^{54}R_{in} = {^{54}k}{^{54}C(t)}$ and $^{56}R_{in} = {^{56}k}{^{56}C(t)}$, respectively we write:

$$\frac{^{54}R_{in}}{^{56}R_{in}} = \frac{\dfrac{^{54}F_{in}}{x}\left(1 - e^{-^{54}kt}\right) + {^{54}k}{^{54}C_0}e^{-^{54}kt}}{\dfrac{^{56}F_{in}}{x}\left(1 - e^{-^{56}kt}\right) + {^{56}k}{^{56}C_0}e^{-^{56}kt}} \tag{9}$$

This function dictates that at t = 0:

$$\frac{^{54}R_{in}}{^{56}R_{in}} = \frac{^{54}k^{54}C_0}{^{56}k^{56}C_0} \tag{10}$$

where $^{54}C_0/^{56}C_0$ is identical to the isotopic ratio in the bulk mineral. Hence, at the beginning of leached layer formation, the isotopic composition of Fe entering solution is fractionated from the bulk mineral composition if $^{54}k \neq {^{56}k}$.

As $t \rightarrow \infty$,

$$\frac{^{54}R_{in}}{^{56}R_{in}} = \frac{^{54}F_{in}}{^{56}F_{in}} \tag{11}$$

Hence, the isotopic composition of Fe entering solution (R_{in}) becomes constant as the leached layer reaches steady-state. This value should equal the isotopic ratio in the bulk material, unless isotope selectivity during diffusion through the leached layer is important. White and Yee (1985) argued that oxidation of Fe at the hornblende surface under aerobic conditions is rate-limited by cation diffusion through the leached layer. Hence, the possibility of such effects cannot be discounted.

The time course of these relationships is illustrated schematically as lines in Figure 6 for two cases. In both cases, for

purposes of illustration we assume $^{54}k/^{56}k = 1.001$ (i.e., the rate constant for ^{54}Fe removal is 1‰ larger than that of ^{56}Fe). One case assumes $F_{in/x} \gg kC_0$ (solid line). In this case, the rate of removal from the surface is limiting, so that C(t) for each isotope varies from C_0 to the steady state value $[F_{in}/(kx)]$. Fractionation in this case is simply governed by the relative magnitude of the removal rate constants until steady-state conditions are established; ($^{54}R_{in}/^{56}R_{in}$)/($^{54}C_0/^{56}C_0$) ($=^{54}k/^{56}k$) is initially 1.001, and descends smoothly to a steady-state value identical to that of the bulk mineral. The rate of descent is controlled by the relative magnitudes of F_{in}, C_0 and k. In contrast, if we assume $F_{in/x} \ll kC_0$ (dashed line), C(t) in the leached layer drops from C_0 because Fe is removed from the layer faster than it is replaced. Because ^{54}Fe leaves faster than ^{56}Fe, this leads to an "overshooting" and a transient ^{56}Fe-enriched isotopic composition in the leached layer. After an initial period when ^{54}Fe enters solution faster than ^{56}Fe, ^{56}Fe then enters more rapidly until steady-state is attained. The magnitude and duration of this transient is governed by the relative magnitudes of F_{in}, C_0 and k. Because the leached layer is observed to be Fe-depleted, the situation $F_{in/x} \ll kC_0$ (dashed line) is most likely.

Importantly, Figure 6 depicts the relative rates of release of ^{54}Fe and ^{56}Fe to solution at any given time, rather than the isotopic composition of the accumulated dissolved Fe, which can only be derived from integrations of these curves. Integrated curves are shown in Figure 7, plotted as $\Delta^{56}Fe_{soln-hbl}$ ($=\delta^{56}Fe_{solution} - \delta^{56}Fe_{hornblende}$). In both cases, the solution is initially enriched in ^{54}Fe relative to the mineral, but evolves toward the isotopic composition of the bulk mineral. This evolution is more rapid when $kC_0 \gg F_{in/x}$. Even for the model with the overshoot, the flux of isotopically heavy Fe entering solution after the "overshoot" is small compared to the amount of Fe previously accumulated in solution, and so the two curves are similar, though with different time constants.

Clearly, the isotopic composition of dissolved Fe can change with time in a mineral dissolution system during formation of
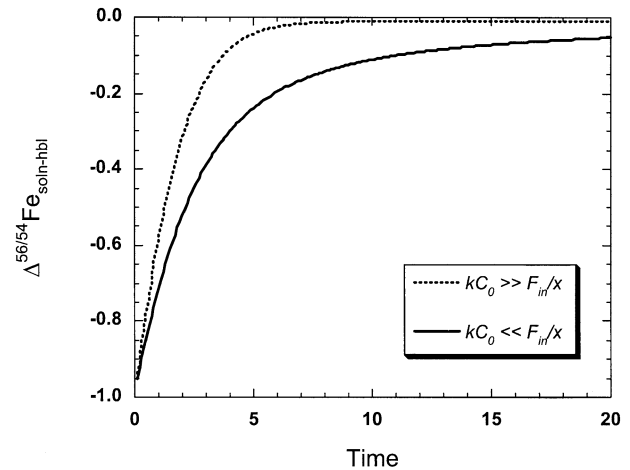

Fig. 7. Offset of $^{56}Fe/^{54}Fe$ between solution and bulk mineral for the two cases shown in Figure 6 ($kC_0 \ll F_{in/x}$, solid line; $kC_0 \gg F_{in/x}$, dotted line). $\Delta^{56}Fe_{soln-hbl} = \delta^{56}Fe_{solution} - \delta^{56}Fe_{hornblende}$. In both cases, an initial fractionation of ~ -1‰ evolves to little or no fractionation as the leached layer approaches steady-state. Units of time are arbitrary.

a surface leached layer, if there is a kinetic isotope effect when Fe is liberated from the mineral.

The kinetic, leached-layer model may also explain the correlation of $\Delta^{56}Fe$ and log (K_{assoc}) (Fig. 5). Assuming reactions such as (3) and (4) go to completion at the surface, Fe transfer to solution will occur as Fe^{3+}-ligand complexes. However, before equilibrium is attained between Fe^{2+} and Fe^{3+} within the altered layer, a kinetic isotope effect could cause an enhanced rate of oxidation of ^{54}Fe vs. that of ^{56}Fe, creating a pool of isotopically light ferric iron at the surface. Eventually, as equilibrium is attained, ferric iron at the surface would become isotopically heavy, but far from equilibrium, surface ferric iron should be isotopically light. Therefore, as long as the rate of loss of ferric ions to solution is faster than the rate at which Fe^{3+} and Fe^{2+} attain equilibrium in the altered layer, ^{54}Fe will accumulate in solution. In contrast, if loss of Fe to solution is slow, the isotopic equilibration between Fe^{2+} and Fe^{3+} within the surface will lead to Fe^{3+} being isotopically heavy, and loss to solution will be enriched in ^{56}Fe. Higher affinity ligands should lead to more rapid transfer of Fe to solution, favoring transfer of Fe to solution at a rate faster than the isotopic equilibration rate. Hence, such ligands should favor the transfer of light Fe to solution, as observed (Fig. 5). Consistent with these arguments, the rate at which Fe accumulates in solution increases as K_{assoc} increases (Fig. 3).

This leached layer model may also account for the puzzling observation of Brantley et al. (2001b) that fractionation in experiments with DFAM and hornblende is smaller after 6 d than after 4 d: the DFAM experiments presumably evolve further toward steady-state between 4 and 6 d. Such evolution was not seen in experiments with oxalic acid, perhaps because the leached layer develops more slowly when the rate of Fe release is lower (Fig. 5).

4.3.2. Goethite experiments

Given the hypothesis that Fe isotope fractionation was caused during the creation of an altered layer on hornblende, we predicted that Fe isotope effects during dissolution of goethite, on which no leached layer develops, would be minimal. As predicted, we observed little to no significant Fe isotope fractionation when goethite was exposed to DFAM (Tables 3 and 5). In abiotic MM9 solution, Fe was not released in large enough concentrations to measure the isotopic signature.

In contrast to these abiotic goethite measurements, Fe isotopes are fractionated during growth of the siderophore-producing Bacillus in the presence of goethite (Tables 3 and 5). Dissolved Fe after 6 d is isotopically light compared to Fe in the mineral. In addition, both ferrous and ferric iron were measured in solution at 4 and 6 d during dissolution in the presence of the bacteria (Table 3, Fig. 4).

Observation of isotopically light aqueous Fe in the presence of the bacteria is consistent with reduction of ferric to ferrous ions as P_{O2} decreases in bacterial experiments, equilibration of ferrous and ferric iron in solution, and bacterial uptake of isotopically heavy ferric iron complexes. Siderophore-Fe^{3+} complexes dock onto the cell membrane where they are either taken up whole into the cytoplasm or are reduced and taken into the cell while the siderophore is recycled (Madigan et al., 2000). Ferrous iron transport systems have been found in

facultative anaerobic bacteria such as Enterobacteriaceae, where ferrous iron transport may contribute to the cellular Fe pool (Braun et al., 1998); however, we found no evidence in the literature for ferrous Fe uptake by aerobic bacteria. Therefore, isotopic fractionation could occur during equilibration of ferrous and ferric iron in solution (see discussion above where α for hydroxo complexes is ~1.0028; Johnson et al., 2002), while bacterial uptake of Fe^{3+} could deplete the solution in ^{56}Fe.

A mass balance calculation can be used to check if this model can explain all observations. Assuming $\Delta^{56}Fe_{FeIII-FeII}$ in solution ($= \delta^{56}Fe_{FeIII} - \delta^{56}Fe_{FeII}$) of 2.75 (Johnson et al., 2002) and that the value of $\delta^{56}Fe$ released to solution during bacterially mediated goethite dissolution $= -0.23‰$ (i.e., Fe released to solution is identical to goethite starting material before significant bacterial growth), and assuming a maximum of 20% ferrous iron in solution during bacterial growth as observed in the presence of goethite (Table 3), we calculate $\delta^{56}Fe_{FeIII(aq)} = 0.33‰$ and $\delta^{56}Fe_{FeII(aq)} = -2.42‰$. This calculation suggests that bacterial pellets, if they take up only Fe^{3+}, should have a maximum isotopic signature of 0.33‰. For reaction flasks at the completion of experiments containing 5 μM total Fe in ~100 mL, ~30 μg Fe remain in solution. The isotopic signature of this final dissolved Fe measured $-1.67‰$ (Table 3), significantly lower than the goethite starting material ($-0.23‰$). Assuming that Fe released from the goethite was isotopically identical to the goethite ($-0.23‰$), then mass balance requires that $\leq$28% of the Fe went into solution ($-1.67‰$) and $\geq$72% went into cells (0.33‰).

Such a mass balance calculation could be verified if cells were analyzed for Fe isotopic compositions in bacilli + goethite experiments. However, cells could not be physically separated from goethite. A rough estimate of cell mass and Fe content can be attempted however. We base this calculation on prior experience with bacillus experiments conducted with 500 mL medium and 7 g of hornblende for ~10 d (Guynn, 2001): cell pellets were collected by centrifugation and separated from mineral grains by Percoll gradient centrifugation. The recovered cells were washed, repelleted, dried at 60°C and weighed. The measured mass of cell pellets in hornblende + bacilli experiments (0.022 ± 0.003 g, average of three runs) was significantly higher than the similar value for bacilli-only experiments (0.006 ± 0.004 g, average of four runs), documenting that cell growth was faster in the presence of the Fe-containing mineral. The mass of Fe in digested cell pellets from the three flasks with hornblende averaged 58 ± 14 μg Fe (Guynn, 2001). This can be compared to the total Fe in solution at the end of the experiment (7 μM in ~500 mL) to calculate the fraction of Fe extracted from the hornblende which was taken up by the bacteria: ~20%. Given that only 20% of the Fe was taken up into bacilli with the hornblende experiments, it is unlikely that the goethite experiments described in this paper yielded a cell pellet that assimilated as much as 72% of the Fe, as required by mass balance to explain the isotopic shift observed for the Fe in solution (see previous paragraph). It is therefore likely that another sink for isotopically heavy Fe must be considered.

As discussed previously, precipitation or adsorption of isotopically heavy Fe are both possibilities for these experiments. However, it is unlikely that precipitation occurs in goethite + bacillus experiments (where fractionation is observed in the

presence of siderophore) but does not occur in goethite + MM9 experiments (where no fractionation is observed and no siderophore is present). Precipitation is therefore considered to be an unlikely explanation for fractionation in goethite + bacillus experiments. In contrast, Figure 2 documents that dissolved Fe decreases, on average, between 4 and 6 d in goethite + bacillus experiments. Such a decrease in aqueous Fe could occur as adsorption removes Fe from solution.

Based upon these considerations, adsorption of isotopically heavy Fe must be considered as a possible mechanism contributing to fractionation. Given that no significant isotopic fractionation was observed for abiotic goethite experiments where no ferrous iron was identified (Table 3), adsorption of Fe^{2+} must be more important than Fe^{3+} onto goethite. The missing sink for isotopically heavy Fe is therefore most likely adsorption of ferrous iron to goethite or bacterial cells. In fact, in abiotic experiments with $FeCl_{2(aq)}$ and goethite, we have observed that significant Fe (30%) is adsorbed by goethite, and that Fe remaining in solution after sorption is isotopically light by ~1‰ (Icopini et al., 2004). Icopini et al. also tested fractionation during Fe adsorption onto Shewanella cells, and observed insignificant fractionation. Testing for adsorption of ferrous iron in experiments reported here was impossible because we were unable to separate bacteria from goethite after growth. However, some evidence for adsorption may be observed in Figure 4: ferrous iron is released quickly from 1 to 4 d and then decreases in concentration in solution, possibly documenting adsorption in the experiment. Adsorption could produce the observed direction of shift in the event of an equilibrium fractionation between dissolved and adsorbed Fe^{2+} favoring adsorption of the heavy isotope. Such a partitioning might be expected if the bonding environment for ferrous iron in solution were significantly weaker than at the mineral interface. Icopini et al. (2004) also inferred that the fractionation effect may be time-dependent, and may be related to reconstruction reactions occurring at the goethite surface.

4.3.3. Weathering

Analysis of our experiments leads to the necessity of hypothesizing three contributing mechanisms for isotopic fractionation during weathering:

1) Incomplete leaching of Fe from an altered layer on silicate releases isotopically light Fe to solution, as documented by the fractionation observed in the DFAM + hornblende experiment, and the lack of fractionation during goethite + DFAM dissolution. The lack of ferrous iron in the DFAM + hornblende experiment precludes fractionation by either mechanisms (2) or (3) below.

2) Isotopic fractionation between aqueous ferrous and ferric ions, followed by uptake of isotopically heavy ferric iron by bacterial cells, depletes ^{56}Fe in solution, as suggested by isotopic fractionation during bacteria growth in the presence of goethite. While mechanism (3) below can also contribute to the isotopic fractionation observed in goethite + Bacillus sp. experiments, mechanism (1) is precluded because no leached layer forms on goethite.

3) Adsorption of isotopically heavy ferrous iron onto goethite enriches isotopically light Fe in solution, as required to explain isotopic mass balance in the goethite + Bacillus sp.

experiments. Mechanisms (2) and (3) may both contribute to the large fractionation observed when goethite is dissolved in the presence of Bacillus.

The isotopic signature of Fe in natural solutions is probably also controlled by the competing reactions of nonstoichiometric mineral dissolution of silicates, bacterial uptake, and adsorption/desorption reactions. In addition, precipitation of isotopically distinct minerals may also contribute to fractionation (Bullen et al., 2001). While geologic systems might be expected to document only equilibrium isotope effects because of the long time periods available for equilibration, kinetic isotopic fractionation can be preserved in the rock record in open systems. In particular, for geologic systems such as soils where fluid flow may serve to separate species with different isotopic signatures, fractionation due to kinetic effects may be preserved.

Of course, some of the effects documented in our experiments are transient: for example, once a weathering hornblende develops a steady state leached layer, the Fe released to solution will become isotopically identical to hornblende starting material. Similarly, adsorption might be expected to become a steady state reservoir within relatively short time periods, given that adsorption generally reaches equilibrium quickly. Furthermore, if soil biota reach a steady state mass and begin to recycle biotic Fe instead of taking up new soil-derived Fe, then fractionation due to that mechanism will also go to zero. However, we are unaware of evidence suggesting whether leached layers on hornblende reach steady state: indeed, Mogk and Locke (1988) argued that leaching of a hornblende grain for more than 100,000 yr did not yield a steady state leached layer. Furthermore, soil biota may or may not attain steady state, and, even if soil biota reach steady state (constant mass with time), Fe within biota may not be at steady state. If Fe is taken up in soil biota and then sequestered into recalcitrant organic matter, this organic matter might become a long-term sink for heavy Fe isotopic material, and Fe in soil solutions might remain isotopically light during ongoing soil development. To understand these phenomena, we need more data concerning which processes contributing to kinetic isotope effects reach steady state and the time to reach steady state. With such information, we could conclude that some processes will not yield isotopic fractionation in the rock record (processes that reach steady state in time periods less than soil age) while other processes yield isotopic fractionations documented in the rock record (processes that do not reach steady state over the lifetime of the soil).

To determine if Fe fractionation is recorded in soil, Brantley et al. (2001b) looked for and documented Fe isotope fractionation in Gore Mountain soil (Soil 1, Table 6). In that measurement, extraction of the most labile Fe fraction from Gore Mountain soil released isotopically light Fe. To verify that observation, two new extractions were performed here in triplicate on another B-horizon soil from Gore Mountain (Soil 2, Table 6). Exchangeable Fe and Fe oxides were removed from the soil using the same procedures as previously (see Methods). As described earlier, quantitative removal of amorphous and crystalline Fe oxides without dissolution of silicates was verified.

Isotopically, $\delta^{56}Fe$ on the cation exchange complex differed by ~1.1‰ from $\delta^{56}Fe$ in oxides in the same soil (Table 6), a

difference similar within error to that reported by Brantley et al. (2001b) for a different soil (Soil 1) from the same site. The low levels of Si present in both the exchangeable and oxide extraction solutions (see "Results" section) indicate that neither of the extraction procedures caused congruent dissolution of silicate minerals. The lack of isotopic difference between the citrate-dithionite solution obtained after incomplete and complete dissolution of goethite (Table 6) documents that citrate-dithionite does not fractionate Fe measurably during extraction. Therefore, the isotopic signature of Fe oxyhydroxides in the Gore Mountain soil (citrate-dithionite extracted) is identical to the hornblende in that soil (Table 6), suggesting that precipitation is not a mechanism causing Fe fractionation in these soils. Similarly, values of δ^{56}Fe measured on $MgCl_2$ extractions completed for different periods of time (Soil 2, sample 2, Table 6) were also identical within error.

These results are consistent with the conclusion that labile Fe on grain surfaces of this spodsol are isotopically lighter than hornblende starting material ($\sim$0‰) or than Fe oxides in the soil ($\sim$0‰). This labile Fe is most likely organically complexed Fe extracted from Fe silicates weathering in the soil. All of the fractionation processes discussed in this paper could contribute to isotopically light Fe in solution and on the exchangeable sites.

5. CONCLUSIONS

Isotopic fractionation of Fe occurs during dissolution of minerals under some circumstances. The causes of the fractionation are complex and varied, including fractionation due to creation of leached layers on Fe-containing aluminosilicate, fractionation between ferrous and ferric ions in solution, fractionation due to uptake of isotopically heavy ferric iron by bacteria, and fractionation during adsorption of ferrous iron onto mineral surfaces. Although not required here, fractionation could also occur due to precipitation of Fe minerals (Bullen et al., 2001).

Based upon the work reported in this paper, the isotopic fractionation reported for hornblende + bacillus experiments (Brantley et al., 2001b) probably resulted from a combination of factors, all contributing to depletion of ^{56}Fe in solution. First, fractionation during formation of the Fe-depleted layer of the silicate surface can occur, releasing ^{54}Fe to solution faster than ^{56}Fe (Figs. 6 and 7). This may provide an explanation for the Fe isotope value-ligand affinity correlation (Fig. 5). Second, equilibration of ferrous and ferric iron in solution leads to isotopic enrichment of ^{56}Fe in the aqueous ferric iron pool. Uptake of this heavy ferric iron from solution by bacterial cells must deplete the solution in ^{56}Fe (note that Brantley et al., 2001b, documented isotopically heavy Fe in some cell pellets). Third, preferential adsorption of ^{56}Fe^{2+} onto hornblende may occur and further deplete the solution in the heavier isotope. Processes involving Fe(II) are not likely to account for the entire effect seen in hornblende experiments because fractionation is also seen in experiments with hornblende and DFAM where no ferrous iron was measured, and because it is not obvious how these processes can explain the ligand effect shown in Figure 5.

In every case of observed fractionation in both goethite and hornblende dissolution reported in this paper, isotopically heavy Fe was depleted in solution, and the mechanism of such fractionation was affected by the presence of organic ligands and bacteria. Whether such effects are recorded in the rock record or in natural systems remains to be elucidated. However, isotopically light Fe found on exchangeable sites on soil surfaces as reported by Brantley et al. (2001b) and here is consistent with our observations that organic molecules extract isotopically light Fe from incongruently dissolving silicates: if such organically bound Fe comprises the mobile Fe in a natural soil solution then exchangeable Fe should be isotopically light, as observed. We conclude that fractionation of Fe isotopes in low-temperature natural systems will be significantly affected by the presence of silicates that dissolve nonstoichiometrically, by the presence of strong chelates including siderophores, by the redox state of the solution, and by the presence of Fe-assimilating organisms.

REFERENCES

Anbar A. D., Roe J. E., Barling J., and Nealson K. H. (2000) Nonbiological fractionation of iron isotopes. *Science* **288,** 126–128.

Anbar A. D., Knab K. A., and Barling J. (2001) Precise determination of mass-dependent variations in the isotopic composition of molybdenum using MC-ICPMS. *Anal. Chem.* **73,** 1425–1431.

Arnold G. L., Weyer S., and Anbar A. D. (2004) Fe isotope variations in natural materials measured using high resolution MC-ICP-MS . *Anal. Chem.* **76,** 322–327.

Beard B. L., Johnson C. M., Cox L., Sun H., Nealson K., and Aguilar C. (1999) Iron isotope biosignatures. *Science* **285,** 1889–1892.

Beard B. L., Johnson C. M., Skulan J. L., Nealson K. H., Cox L., and Sun H. (2003) Application of. Fe isotopes to tracing the geochemical and biological cycling of Fe. *Chem. Geol.* **195,** 87–117.

Bethke C. M. (2002) *The Geochemists Workbench*. University of Illinois.

Brantley S. L. and Chen Y. (1995) Chemical weathering rates of pyroxenes and amphiboles. In *Chemical Weathering Rates of Silicate Minerals, Vol. 31* (eds. A. F. White and S. L. Brantley), pp. 119–172. Mineralogical Society of America.

Brantley S. L., Liermann L. J., Bau M., and Wu S. (2001a) Uptake of trace metals and rare earth elements from hornblende by a soil bacterium. *Geomicrobiol. J.* **18,** 37–61.

Brantley S. L., Liermann L. J., and Bullen T. D. (2001b) Fractionation of. Fe isotopes by soil microbes and organic acids. *Geology* **29,** 535–538.

Braun V., Hantke K., and Koster W. (1998) Bacterial iron transport: Mechanisms, genetics, and regulation. *In Metal Ions in Biological Systems,* Vol. 35, *Iron Transport and Storage in Microorganisms, Plants, and Animals* (eds. A. Sigel and H. Sigel). pp. 67–146. Marcel Dekker.

Bullen T. D., White A. F., Childs C. W., Vivit D. V., and Schulz M. S. (2001) Field and laboratory evidence of an abiotic iron isotope fractionation mechanism. *Geology* **29,** 699–702.

Buss H. L., Brantley S. L., and Liermann L. J. (2003) Nondestructive methods for removal of bacteria from silicate surfaces. *Geomicrobiol. J.* **20,** 25–42.

Delany J. M. and Lundeen S. R. (1991) The LLNL Thermochemical Data Base–Revised Data and File Format for the EQ3/6 Package, pp. 59. Yucca Mountain Site Characterization Project, Department of Energy.

Fox T. R. (1990) Low-molecular-weight organic acids in selected forest soils of the southeastern USA. *Soil Sci. Soc. Am. J.* **54,** 1139–1144.

Frogner P. and Schweda P. (1998) Hornblende dissolution kinetics at 25°C. *Chem. Geol.* **151** (*1–4*), 169–179.

Guynn R. (2001) Fe release and isotopic fractionation during dissolution of solid substrates in the presence of soil bacteria and organic ligands. M.S. thesis. Pennsylvania State University.

Hendershot W. H., Lalande H., and Duquette M. (1993) Ion exchange and exchangeable cations. *In Soil Sampling and Methods of Analysis* (ed. M. R. Carter), pp. 167–175. Lewis.

Hersman L., Lloyd T., and Sposito G. (1995) Siderophore-promoted dissolution of hematite. *Geochim. Cosmochim. Acta* **59,** 3327–3330.

Hider R. C. (1984) Siderophore mediated absorption of Fe. In *Structure and Bonding, Vol. 58*, pp. 25–87. Springer Verlag.

Hughes M. N. and Poole R. K. (1989) *Metals and Microorganisms.* Chapman and Hall.

Icopini G. A., Ruebush S. S., Tien M., Anbar A. D., and Brantley S. L. (2004) Iron isotope fractionation during microbial reduction of iron: The importance of adsorption. *Geology* **32,** (*3*), 205 –208.

Johnson C. M., Skulan J. L., Beard B. L., Sun H., Nealson K. H., and Braterman P. S. (2002) Isotopic fractionation between Fe(III) and Fe(II) in aqueous solutions. *Earth Planet. Sci. Lett.* **195,** 141–153.

Kalinowski B. E., Liermann L. J., Brantley S. L., Barnes A., and Pantano C. G. (2000a) X-ray photoelectron evidence for bacteria-enhanced dissolution of hornblende. *Geochim. Cosmochim. Acta* **64,** 1331–1343.

Kalinowski B. E., Liermann L. J., Givens S., and Brantley S. L. (2000b) Rates of bacteria-promoted solubilization of Fe from minerals: A review of problems and approaches. *Chem. Geol.* **169,** 357–370.

Kingston H. M. and Walter P. J. (1995) Microwave assisted acid digestion of siliceous and organically based matrices. EPA Draft Method 3052 (SW-846, update III).

Kraemer S. M., Cheah S.-F., Zapf R., Xu J., Raymond K. N., and Sposito G. (1999) Effect of hydroxamate siderophores on Fe release and Pb(II) adsorption by goethite. *Geochim. Cosmochim Acta* **63,** 3003–3008.

LaKind J. S. and Stone A. T. (1989) Reductive dissolution of goethite by phenolic reductants. *Geochimica Cosmochemica Acta* **53,** 961–971.

Langmuir D. and Whittemore D. O. (1971) Variations in the stability of precipitated ferric oxyhydroxides. In *Nonequilibrium Systems in Natural Water Chemistry, Vol. 106*, pp. 209–234. American Chemical Society.

Liermann L. J., Kalinowski B. E., Brantley S. L., and Ferry J. G. (2000a) Role of bacterial siderophores in dissolution of hornblende. *Geochim. Cosmochim. Acta* **64,** 587–602.

Liermann L., Barnes A. S., Kalinowski B. E., Zhou X., and Brantley S. L. (2000b) Microenvironments of pH in biofilms grown on dissolving silicate surfaces. *Chem. Geol.* **171,** 1–16.

Liu C., Zachara J., Gorby Y. A., Szecsody J. E., and Brown C. F. (2001) Microbial reduction of Fe(III) and Sorption/Precipitation of Fe(II) on *Shewanella putrefaciens* Strain CN32. *Environ. Sci. Technol.* **35,** 1385–1393.

Lovely D. R. and Phillips E. J. P. (1986) Availability of ferric iron for microbial reduction in bottom sediments of the freshwater tidal Potomac River. *Appl. Environ. Microbiol.* **52,** 751–757.

Macrellis H. M., Trick C. G., Rue E. L., Smith G., and Bruland K. W. (2001) Collection and detection of natural iron-binding ligands from seawater. *Mar. Chem.* **76,** 175–187.

Madigan M. T., Martinko J. M., and Parker J. (2000) Brock Biology of Microorganisms. Prentice-Hall.

Maniatis T., Fritsch E. F., and Sambrook J. (1982) *Molecular Cloning.* Cold Spring Harbor Laboratory Press.

Maréchal C. N., Télouk P., and Albarède F. (1999) Precise analysis of copper and zinc isotopic compositions by plasma-source mass spectrometry. *Chem. Geol.* **156,** 251–273.

Matthews A., Zhu X. K., and O'Nions K. (2001) Kinetic iron stable isotope fractionation between iron (-II) and (-III) complexes in solution. *Earth Planet. Sci. Lett.* **5936,** (*1*), 1–12.

Mehra O. P. and Jackson M. L. (1960) Iron oxide removal from soils and clays by a dithionite-citrate system buffered with sodium bicarbonate. *Clays Clay Min. 7th Nat. Conf.,* pp. 317–327.

Mogk D. W. and Locke W. W. (1988) Application of auger electron spectroscopy (AES) to naturally weathered hornblende. *Geochim. Cosmochim. Acta* **52,** 2537–2542.

Neilands J. B. (1984) Methodology of siderophores. In *Structure and Bonding, Vol. 58*, pp. 1–24. Springer Verlag.

NIST. (1998) *NIST Critically Selected Stability Constants of Metal Complexes Database.* U.S. Department of Commerce.

Powell P. E., Cline G. R., Reid C. P. P., and Szaniszlo P. J. (1980) Occurrence of hydroxamate siderophore iron chelators in soils. *Nature* **287,** 833–834.

Reid R. T., Live D. H., Faulkner D. J., and Butler A. (1993) A siderophore from a marine bacterium with an exceptional ferric ion affinity constant. *Nature* **366,** 455–458.

Roe J. D., Anbar A. and Barling J. (2003) (195) Nonbiological fractionation of Fe isotopes: Evidence of an equilibrium isotope effect. *Chem. Geol.* 69–85.

Rue E. L. and Bruland K. W. (1997) The role of organic complexation on ambient iron chemistry in the equatorial Pacific Ocean and the response of a mesoscale iron addition experiment. *Limnol. Oceanogr.* **42,** 901–910.

Schauble E. A., Rossman G. R., and Taylor H. P., Jr.. (2001) Theoretical estimate of equilibrium Fe-isotope fractionations from vibrational spectroscopy. *Geochim. Cosmochim. Acta* **65,** 2487–2497.

Schwertmann A. and Cornell R. M. (1991) *Iron Oxides in the Laboratory: Preparation and Characterization.* Wienheim.

Schwyn B. and Neilands J. B. (1987) Universal chemical assay for the detection and determination of siderophores. *Anal. Biochem.* **160,** 47–56.

Sharma M., Polizzotto M. L., and Anbar A. D. (2001) Iron isotopes in hydrothermal fluids at the Juan de Fuca ridge. *Earth Planet. Sci. Lett.* **194,** 39–51.

Skulan J. L., Beard B. L., and Johnson C. M. (2002) Kinetic and equilibrium Fe isotope fractionation between aqueous Fe(III) and hematite. *Geochim. Cosmochim. Acta* **66,** 2995–3015.

Stone A. T. (1997) Reactions of extracellular organic ligands with dissolved metal ions and mineral surfaces. In *Geomicrobiology: Interactions between Microbes and Minerals, Vol. 35* (eds. J. F. Banfield and K. H. Nealson), pp. 309–344.

Stumm W. and Sulzberger B. (1992) The cycling of iron in natural environments; considerations based on laboratory studies of heterogeneous redox processes. *Geochim. Cosmochim. Acta* **56,** 3233–3257.

Suter D., Siffert C., and Sulzberger (1998) Catalytic dissolution of Iron (III) (Hydr)oxides by oxalic-acid in the presence of Fe(II). *Naturwissenschaften* **75,** (*11*), 571–573.

Urey H. C. (1947) The thermodynamic properties of isotopic substances. *J. Chem. Soc.* 562–581.

Watteau F. and Berthelin J. (1994) Microbial dissolution of iron and aluminum from soil minerals: Efficiency and specificity of hydroxamate siderophores compared to aliphatic acids. *Eur. J. Soil Biol.* **30,** 1–9.

Weyer S. and Schweiters J. B. (2003) High precision. Fe isotope measurements with high mass resolution MC-ICPMS. *Int. J. Mass Spect.* **226,** 355–368.

White A. F. and Yee A. (1985) Aqueous oxidation-reduction kinetics associated with coupled electron-cation transfer from iron-containing silicates at 25°C. *Geochim. Cosmochim. Acta* **42,** 1075–1090.

White A. F. and Brantley S. L. (1995) *Chemical Weathering Rates of Silicate Minerals.* Mineralogical Society of America.

Winkelmann G. (1991) Specificity of iron transport in bacteria and fungi. In *CRC Handbook of Microbial Iron Chelates,* p. 366. CRC Press.

Zhu X. K., Guo Y., Williams R. J. P., O'Nions R. K., Matthews A., Belshaw N. S., Canters G. W., de Waal E. C., Weser U., Burgess B. K., and Salvato B. (2002) Mass fractionation processes of transition metal isotopes. *Earth Planet. Sci. Lett.* **200,** 47–62.